Backward Lasing of Air plasma pumped by Circularly polarized femtosecond pulses for the saKe of remote sensing (BLACK)

Pengji Ding, Sergey Mitryukovskiy, Aurélien Houard, Eduardo Oliva, Arnaud Couairon, André Mysyrowicz, Yi Liu

Backward Lasing of Air plasma pumped by Circularly polarized femtosecond pulses for the saKe of remote sensing (BLACK)

Pengji Ding[1], Sergey Mitryukovskiy[1], Aurélien Houard[1], Eduardo Oliva[2],
Arnaud Couairon[3], André Mysyrowicz[1], and Yi Liu[1],*

[1] *Laboratoire d'Optique Appliquée, ENSTA ParisTech/CNRS/Ecole Polytechnique, 828, Boulevard des Maréchaux, Palaiseau, F-91762, France*
[2] *Laboratoire de Physique des Gaz et des Plasmas, Université Paris Sud/CNRS, Orsay, F-91405, France*
[3] *Centre de Physique Théorique, Ecole Polytechnique, CNRS, Palaiseau, F-91128, France*
yi.liu@ensta-paristech.fr

Abstract: Recently, S. Mitryukovskiy *et al*. presented experimental evidence showing that backward Amplified Spontaneous Emission (ASE) at 337 nm can be obtained from plasma filaments in nitrogen gas pumped by circularly polarized 800 nm femtosecond pulses (Opt. Express, **22**, 12750 (2014)). Here, we report that a seed pulse injected in the backward direction can be amplified by ~ 200 times inside this plasma amplifier. The amplified 337 nm radiation can be either linearly or circularly polarized, dictated by the seeding pulse, which is distinct from the non-polarized nature of the ASE. We performed comprehensive measurements as to the spatial profile, optical gain dynamics, and seed pulse energy dependence of this amplification process. These measurements allow us to deduce the pulse duration of the ASE and the amplified 337 nm radiation and the corresponding laser intensity inside the plasma amplifier, which indicates that the amplification is largely in the unsaturated regime and further improvement of laser energy is possible. Moreover, we observed an optical gain in plasma created in ambient air, which is of great importance for the future application of this scheme of backward lasing in remote sensing.

OCIS codes: (190.7110) Ultrafast nonlinear optics; (140.4130) Molecular gas lasers.

References and links

1. A. Dogariu, J. B. Michael, M. O. Scully, and R. B. Miles, "High-gain backward lasing in air," Science **331**(6016), 442-445 (2011).
2. Q. Luo, W. Liu, and S. L. Chin, "Lasing action in air induced by ultra-fast laser filamentation," Appl. Phys. B **76**(3), 337-340 (2003).
3. D. Kartashov, S. Ališauskas, G. Andriukaitis, A. Pugžlys, M. Shneider, A. Zheltikov, S. L. Chin, and A. Baltuška, "Free-space nitrogen gas laser driven by a femtosecond filament," Phys. Rev. A **86**(3), 033831 (2012).
4. P. R. Hemmer, R. B. Miles, P. Polynkin, T. Siebert, A. V. Sokolov, P. Sprangle, and M. O. Scully, "Standoff spectroscopy via remote generation of a backward-propagating laser beam," Proc. Nat. Acad. Sci. USA **108**(8)**,** 3130-3134 (2011).
5. P. Sprangle, J. Peñano, B. Hafizi, D. Gordon, and M. Scully, "Remotely induced atmospheric lasing," Appl. Phys. Lett. **98**(21), 211102 (2011).
6. J. Peñano, Ph. Sprangle, B. Hafizi, D. Fordon, R. Fernsler, and M. Scully, "Remote lasing in air by recombination and electron impact excitation of molecular nitrogen," J. Appl. Phys. **111**(3), 033105 (2012).
7. S. Mitryukovskiy, Y. Liu, P. J. Ding, A. Houard, A. Mysyrowicz, "Backward stimulated radiation from filaments in nitrogen gas and air pumped by circularly polarized 800 nm femtosecond laser pulses," Opt. Express **22**(11), 12750-12759 (2014).
8. J. Yao, H. Xie, B. Zeng, W. Chu, G. Li, J. Ni, H. Zhang, C. Jing, C. Zhang, H. Xu, Y. Cheng, and Z. Xu, "Gain dynamics of a free-space nitrogen laser pumped by circularly polarized femtosecond laser pulses," Opt. Express, **22**(16), 19005 (2014).

9. J. Yao, B. Zeng, H. Xu, G. Li, W. Chu, J. Ni, H. Zhang, S. L. Chin, Y. Cheng, and Z. Xu, "High-brightness switchable multiwavelength remote laser in air," Phys. Rev. A **84**(5), 051802(R) (2011).

10. J. Yao, G. Li, C. Jing, B. Zeng, W. Chu, J. Ni, H. Zhang, H. Xie, C. Zhang, H. Li, H. Xu, S. L. Chin, Y. Cheng, and Z. Xu,, "Remote creation of coherent emissions in air with two-color ultrafast laser pulses," New J. Phys. **15**(2), 023046 (2013).

11. Y. Liu, Y. Brelet, G. Piont, A. Houard, and A. Mysyrowicz, "Self-seeded lasing action of air pumped by 800 nm femtosecond laser pulses," Opt. Express **21**(19), 22791-22798 (2013).

12. T. Wang, J. Ju, J. F. Daigle, S. Yuan, R. Li, and S. L. Chin, "Self-seeded forward lasing action from a femtosecond Ti: Sapphire laser filament in air," Las. Phys. Lett. **10**(12), 125401 (2013).

13. D. Kantashov, S. Ališauskas, A. Baltuška, A. Schmitt-Sody, W. Roach, and P. Polynkin, "Remotely pumped stimulated emission at 337 nm in atmospheric nitrogen," Phys. Rev. A **88**(4), 041805 (R) (2013).

14. G. Point, Y. Liu, Y. Brelet, S. Mitryukovskiy, P. J. Ding, A. Houard, and A. Mysyrowicz, "Lasing of ambient air with microjoule pulse energy pumped by a multi-terawatt femtosecond laser," Opt. Lett. **39**(7), 1725-1728 (2014).

15. G. Li, C. Jing, B. Zeng, H. Xie, J. Yao, W. Chu, J. Ni, H. Zhang, H. Xu, Y. Cheng, and Z. Xu, "Signature of superradiance from a nitrogen-gas plasma channel produced by strong-field ionization," Phys. Rev. A **89**(3), 033833 (2014).

16. P. N. Malevich, D. Kartashov, Z. Pu, S. Ališauskas, A. Pugžlys, A. Baltuška, L. Giniūnas, R. Danielius, A. A. Lanin, A. M. Zheltikov, M. Marangoni, and G. Cerullo, "Ultrafast-laser-induced backward stimulated Raman scattering for tracing atmospheric gases," Opt. Express, **20**(17), 18784-18794 (2012).

17. D. Kartashov, P. Malevich, R. Maurer, S. Ališauskas, M. Marangoni, G. Cerullo, A. Zheltikov, A. Pugžlys, and A. Baltuška, "Mirrorless backward SRS in free-space gas driven by filament-initiated UV laser," International Conference on Ultrafast Phenomena, Okinawa, Japan, 2014.

18. R. S. Kunabenchi, M. R. Gorbal, and M. I. Savadatt, "Nitrogen lasers," Prog. Quantum Electron. **9**(4), 259-329 (1984).

19. A. Hariri and S. Sarikhani, "Amplified spontaneous emission in N2 lasers: Saturation and bandwidth study," Opt. Commun. **318**, 152-161 (2014).

20. X. M. Zhao, J. C. Diels, C. Y. Wang, and J. M. Elizondo, "Femtosecond ultraviolet laser pulse induced lightning discharges in gases," IEEE J. Quantum Electron. **31**(3), 599–612 (1995).

21. J. T. Fons, R. S. Schappe, and C. C. Lin, "Electron-impact excitation of the second positive band system ($C^3\Pi_u \rightarrow B^3\Pi_g$) and the $C^3\Pi_u$ electronic state of the nitrogen molecule," Phys. Rev. A **53**(4), 2239-2247 (1996).

22. P. Corkum and N. H. Burnett, in OSA Proceedings on Short Wavelength Coherent Radiation: Generation and Applications,edited by R. W. Falcone and J. Kirz (Optical Society of America, Washington, DC, 1988), **2**, page 255.

23. Ph. Zeitoun, G. Faivre, S. Sebban, T. Mocek, A. Hallou, M. Fajardo, D. Aubert, Ph. Balcou, F. Burgy, D. Douillet, S. Kazamias, G. de Lachèze-Murel, T. Lefrou, S. le Pape, P. Mercère, H. Merjji, A. S. Morlens, J. P. Rousseau, and C. Valentin, "A high intensity highly coherent soft X-ray femtosecond laser seeded by a high harmonic beam," Nature, **431**, 426-429 (2004).

24. S. Sebban, R. Haroutunian, Ph. Balcou, G. Grillon, A. Rousse, S. Kazamias, T. Marin, J. P. Rousseau, L. Notebaert, M. Pittman, J. P. Chambaret, A. Antonetti, D. Hulin, D. Ros, A. Klisnick, A. Carillon, P. Jaeglé, G. Jamelot, and J. F. Wyart, "Saturated Amplification of a Collisionally Pumped Optical-Field-Ionization Soft X-Ray Laser at 41.8 nm," Phys. Rev. Lett. **86**(14), 3004-3007 (2001).

25. I. R. AlMiev, O. Larroche, D. Benredjem, J. Dubau, S. Kazamias, C. Moller, and A. Klisnick, "Dynamial descriptin of transient X-ray lasers seeded with high-order harmonic radiation through Maxwell-Bloch numerical simulations," Phys. Rev. Lett. **99**, 123902 (2007).

26. E. Oliva, Ph. Zeitoun, M. Fajardo, G. Lambert, D. Ros, S. Sebban, and P. Velarde, "Comparison of nature and forced amplification regimes in plasma-based soft-x-ray lasers seeded by high-order harmonics," Phys. Rev. A, **84**(1), 013811 (2011).

27. T. Tabata, T. Shirai, M. Sataka, H. Kubo, "Analytic cross sections for electron impact collisions with nitrogen molecules," At. Data Nucl. Data Tables **92**(3), 375–406 (2006).

1. Introduction

Stimulated radiation of air plasma pumped by ultrashort intense laser pulses has attracted growing attention in recent 3 years [1-15]. Both backward and forward stimulated emission has been observed in experiments. In particular, the backward stimulated emission is very interesting, because it can be potentially employed for remote sensing applications. The employment of a backward stimulated lasing radiation for remote sensing is expected to bring tremendous improvement of measurement precision and sensitivity, because coherent

detection methods such as Stimulated Raman Scattering (SRS) can be then used instead of the incoherent detection of laser induced luminescence [16, 17].

Up to now, two different schemes of backward lasing action have been demonstrated. In the first method, a picosecond ultraviolet (UV) pulse (226 nm) was used to excite oxygen molecules in ambient air [1]. Population inversion between the $3p^3P$ and the $3s^3S$ states of oxygen atom was achieved by two photon dissociation of the oxygen molecules followed by resonant excitation of the atomic oxygen fragments. Both backward and forward stimulated emission at 845 nm has been observed in the experiments. However, application of this scheme for backward lasing generation for remote sensing is difficult due to the poor transmission of the UV pump pulse in atmosphere. Another scheme is based on population inversion in neutral nitrogen molecules. Backward stimulated emission from neutral nitrogen molecules inside a laser plasma filament was first suggested in 2003, based on the observed exponential increase of the backward UV emission with the filament length [2]. In 2012, D. Kartashov and coworkers focused a mid-infrared femtosecond laser pulse (3.9 μm or 1.03 μm) inside a high pressure mixture of argon and nitrogen gas. Backward stimulated emissions at 337 nm and 357 nm were observed with an optimal argon gas pressure of 5 bar and nitrogen pressure of 2 bar [3]. The emission at 337 nm and 357 nm have been identified as being due to the transition between the third and second excited triplet states of neutral nitrogen molecules, i.e. $C^3\Pi_u \rightarrow B^3\Pi_g$. The population inversion mechanism between the $C^3\Pi_u$ and $B^3\Pi_g$ states was attributed to the traditional Bennet mechanism, where collisions transfer the excitation energy of argon atoms to molecular nitrogen [18]. Unfortunately, this method cannot be applied for remote generation of backward lasing emission because of its requirement of high pressure argon gas ($p > 3$ bar).

A few months ago, S. Mitrykovskiy et al. showed that a backward Amplified Spontaneous Emission (ASE) at 337 nm can be obtained from laser filaments in nitrogen gas or its mixture with oxygen pumped by circularly polarized 800 nm femtosecond laser pulses [7]. We there hence acronymize this scheme of backward lasing as BLACK (Backward Lasing of Air Plasma pumped by Circularly polarized femtosecond pulses for the saKe of remote sensing). Very recently, Yao et al measured the gain dynamics of this free-space laser at 337 nm by sending a weak seed pulse in the forward direction and examining the amplified signal as a function of the delay between the pump and the seed pulse. Their study confirmed the existence of population inversion and revealed a gain lifetime around ~ 20 ps in 1 bar nitrogen gas [8].

In this paper, we report that an external seed pulse around 337 nm in the backward direction can be amplified by ~ 200 times inside the plasma amplifier. The divergence of the amplified 337 nm emission is found to be significantly reduced compared to that of ASE. Moreover, the amplified lasing radiation inherits the polarization of the seed pulse. These three observations confirm unambiguously our previous assumption of population inversion between the relevant nitrogen molecular states. We further examined the gain dynamics at different gas pressure, the dependence of the amplified lasing signal on seed pulse energy, and the role of the pump laser ellipticity on the lasing action. With the measured gain lifetime, we are able to estimate the pulse duration of the backward ASE and the amplified 337 nm emission. The 337 nm laser intensity inside the plasma amplifier is then calculated, indicating that the current experiments are in the unsaturated amplification regime. As a result, further increase of the backward laser energy is possible by using higher energy pump or seeding pulse. We also observed amplification of seeding pulses in air plasma created by circularly polarized femtosecond pulses, which confirms that population inversion between the $C^3\Pi_u$ and $B^3\Pi_g$ states can be achieved in ambient air. This opens up the door for practical application of this BLACK scheme for generation of backward lasing in ambient air. Finally, we discussed the mechanism for population inversion, in analogy with the well-developed collisionally pumped X-ray laser amplifier.

2. Experimental setup

In our experiment, a commercial Chirped Pulses Amplification (CPA) laser system (Thales Laser, Alpha 100) was used. This system delivers 42 fs laser pulses at a repetition rate of 100 Hz, with maximum pulse energy of 12 mJ. Two experimental configurations have been employed. In the first scheme, the pump IR pulse and the seed pulse counter-propagate. A schematic experimental setup is presented in Fig. 1. The output laser pulse was split into a main pump pulse and a much weaker second pulse by a 1 mm thick 5%/95% beamsplitter. The pump pulse passed through a $\lambda/4$ waveplate and then was focused by an $f = 1000$ mm convex lens (L_1). A dichromatic mirror was used to reflect the focused 800 nm pump pulses into a gas chamber filled with pure nitrogen gas at 1 bar pressure. This dichromatic mirror reflects more than 99% of the 800 nm pump pulse and it is transparent to the backward ultraviolet emission from the laser plasma situated inside the gas chamber. The second weaker 800nm pulse first passed through a mechanical delay line and then through a 1 mm thick type-I BBO crystal in order to generate femtosecond pulses at 400 nm. The 400 nm pulse was linearly polarized in the vertical direction. The obtained 400 nm pulse was further focused by an $f = 100$ mm convex lens (L_2) inside a 20 mm long fused silica sample to broaden its spectrum through intense nonlinear interaction. We selected the spectrum component around 337 nm with an interference bandpass filter, which has a transmission peak at 337 nm and a bandwidth of 10 nm. The resulting pulse centered at 337 nm, referred to as seeding pulse in the following, was focused by another $f = 100$ mm lens into the gas chamber from the opposite direction of the pump pulses. The separation between the lenses L_2 and L_3 was adjusted to insure that the geometrical focus of the seeding pulse overlapped with the central part the of the long plasma filament in the longitudinal direction. The transverse spatial overlapping between the geometrical focus of the seeding pulse and the center of the plasma filament was carefully assured by translating finely the focal lens (L_3) in the transverse plane. The temporal delay between the 800 nm pump pulses and the seeding pulse at 337 nm could be adjusted by the mechanical delay line. For some of our experiments, we installed a $\lambda/4$ waveplate for 400 nm radiation after the BBO crystal so that a circularly polarized seeding pulse could be obtained after filamentation inside the fused silica sample. The backward emission from the laser plasma filaments was detected by either a spectrometer (Ocean Optics HR 4000), an intensified Charge Coupled Device (iCCD) camera (Princeton Instrument, model: PI-MAX), a calibrated photodiode, or a sensitive laser power meter (model: OPHIR, NOVA, PE9-C).
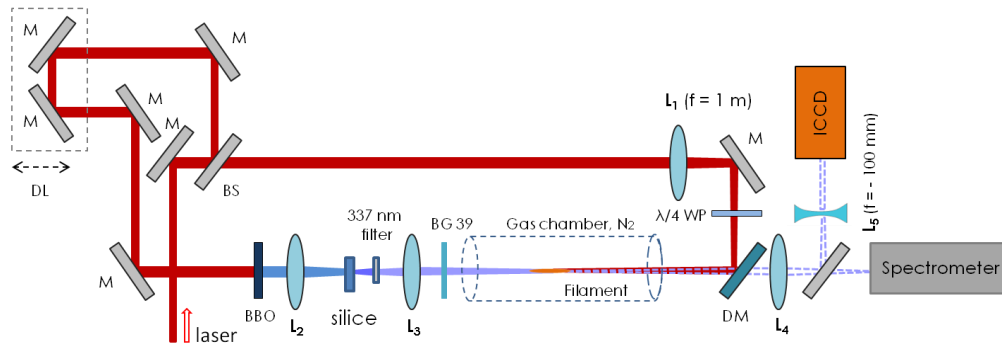

Fig. 1. Schematic experimental setup.

In a second scheme to measure the temporal dynamics of the optical gain of the plasma amplifier, the seed pulse and the pump pulse were arranged to propagate in the same direction. The spatial overlap of the plasma amplifier and the focus zone of the seed pulse was carefully assured. The temporal delay between them was also varied by a mechanical delay line. The analysis of the 337 nm radiation was performed in the downstream of the filament amplifier.

3. Experimental results and discussion

3.1 Manifestation of spectrum narrowing and seed amplification

We first measured the spectra of the backward emissions from the laser plasma without the seed pulse. With pump pulse energy of 8.5 mJ, a 3 cm long filament is formed [7]. In Fig. 2, we present the backward emission spectra for circularly and linearly polarized pump pulses. The emission peaks around 315 nm, 337 nm, 357 nm, 380 nm have been well indentified as the transition between the $C^3\Pi_u$ and $B^3\Pi_g$ states of the neutral nitrogen molecules with different initial and final vibrational quantum numbers, which has been denoted in Fig. 2. The tremendously increased radiation at 337 nm with circular laser polarization suggests occurrence of stimulated emission, referred to as ASE in our previous work [7]. Thanks to a better spectral resolution, a clear spectrum narrowing of the 337 nm radiation in case of lasing is noticeable, which is a common feature of lasing emission compared to spontaneous one. The 337 nm laser bandwidth was measured to be 1.06 nm, which corresponds to the spectral resolution of our spectrometer. Please note that the bandwidth corresponding to the transition between the $C^3\Pi_u$ and $B^3\Pi_g$ state is well known to be around ~ 0.1 nm [19].
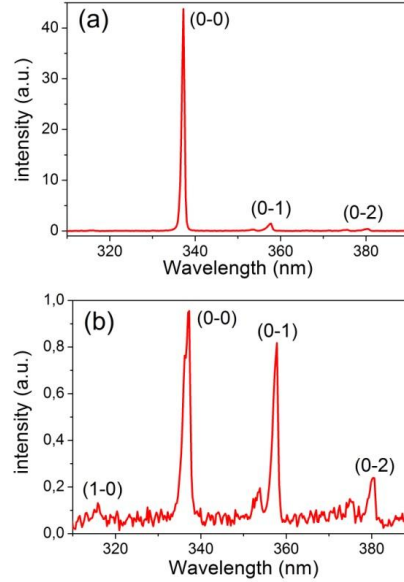

Fig. 2. Backward emission spectrum with circularly (a) and linearly (b) polarized pump pulses. The numbers in the parenthesis denote the vibration quantum number of the initial and final states of the transition.

The backward emission spectra in the presence of the seeding pulses are presented in Fig. 3. Considering the intensity of the seed pulse at the 337 nm spectral position, we estimated that the seed pulse is amplified by a factor of ~ 200 times (Fig. 3 (a)). Compared to the backward ASE, the amplified 337 nm laser emission energy was 40 times higher. With an effective amplifier length of 4.5 mm, we estimated the small-signal gain coefficient to be $g = \ln(I_f/I_0)/l_{eff} = 11.8$ cm^{-1}. Here I_f, I_0, l_{eff} are the intensity of the amplified 337 nm emission, the intensity of the seeding pulse, and the effective length of the plasma amplifier. The effective length of the amplifier is different from the geometrical filament length for the backward ASE and will be discussed later. The population inversion density is then estimated as $\Delta n = g/\sigma_s \sim 10^{15}$ cm^{-3}, where $\sigma_s \sim 10^{-14}$ cm^2 is the stimulated cross-section of the $C^3\Pi_u \rightarrow B^3\Pi_g$ transition [5, 6]. In the case of linearly polarized pump pulses (Fig. 3 (b)), no detectable ASE was observed and no amplification of the seed pulse could be observed.
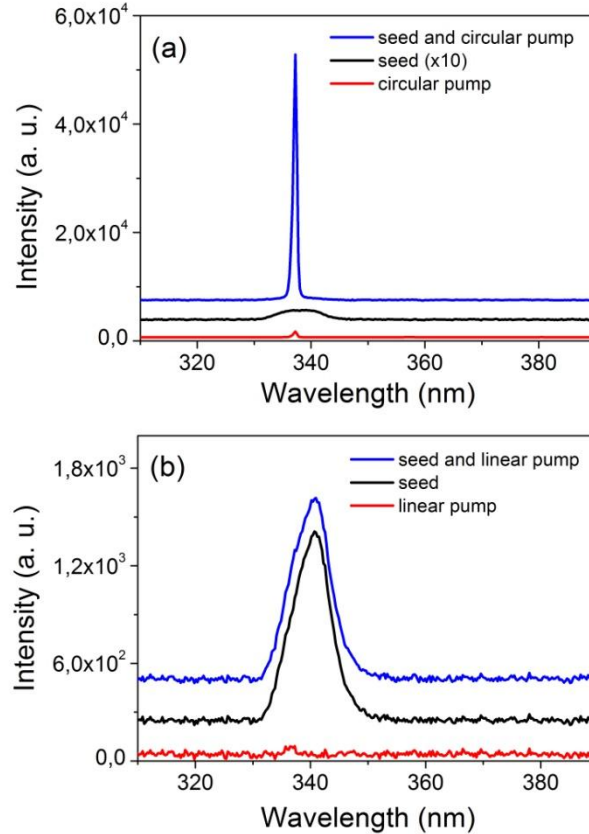
Fig. 3. Spectra of the backward emission with circularly (a) and linearly (b) polarized pump pulsed at 800 nm. The spectra of the seed pulses and those of the backward emission from the pump pulses are also presented for comparison. In (a), the spectrum of the seed pulse is magnified by a factor of 10 for visibility.

3.2. Polarization of the ASE and the amplified 337 nm radiation

We then studied the polarization of the backward ASE and the amplified 337 nm emission. In order to analysis the polarization properties of the lasing radiation, we installed a Glan-Taylor prism before the detecting photodiode. In the experiment, we recorded the intensity of the transmitted 337 nm radiation as a function of the rotation angle of the Glan-Taylor prism. The result for the ASE obtained without seed pulse is presented in Fig. 4 (a), indicating that the ASE is not polarized.
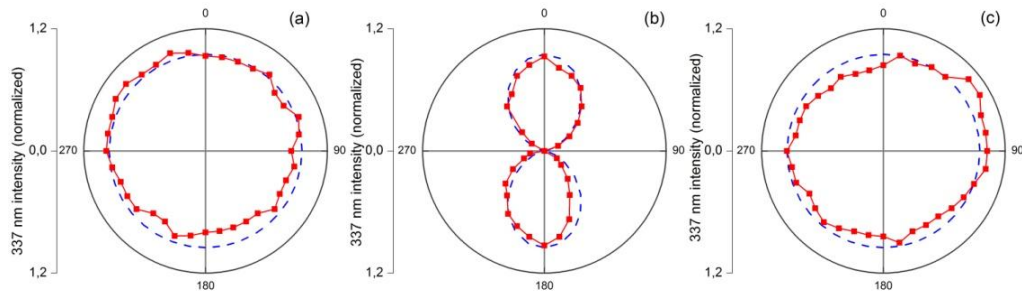

Fig. 4. Polarization of the ASE (a), the seeded backward stimulated emission with linearly (b) and circularly (c) polarized seed pulses at 337 nm. The dots present the experimental results and the dashed lines denote the theoretical fitting.

For linearly polarized seed pulses in the vertical direction, we observed that the amplified lasing signal is also linearly polarized in the same direction (see Fig. 4 (b)), evidenced by the good agreement between the experimental results and the theoretical fit with Malus' law. The result for circularly polarized seeding pulses is presented in Fig. 4 (c), where a circularly polarized amplified emission is also observed. The maintenance of the pulse polarization during the amplification is in agreement with our hypothesis that that population inversion is present and responsible for the seed pulse amplification.

3.3 Spatial profile of the ASE and the amplified 337 nm emission

We measured the spatial profiles of the ASE and the amplified lasing emission with the iCCD camera. In Fig. 5 (a), the spatial profile of the backward ASE is shown. The ASE exhibits a Gaussian distribution with a divergence of 9.2 mrad. In the case of linearly polarized 800 nm pump pulse, no backward emission at 337 nm was observed with the iCCD. We present the spatial profile of the seed pulse in Fig. 5 (b). In the presence of both pump and seed pulse, an extremely intense 337 nm radiation was found, as presented in Fig. 5 (c). This amplified stimulated emission shows a divergence angle of ~ 3.8 mrad, much smaller than that of the ASE and the seed pulse.
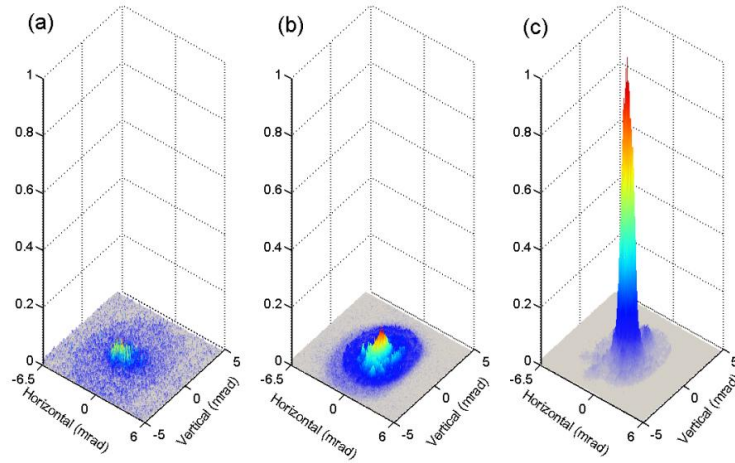

Fig. 5. Spatial profile of the backward ASE (a), the seed pulse (b), and the amplified 337 nm radiation (c). The opening angle of each panel is 12.5 mrad × 10 mrad.

3.4 Seed pulse energy dependence

In order to determine whether the optical amplification is in the saturated regime, we tuned the energy of the seed pulse with a variable metallic optical density. The result is presented in Fig. 6. For this measurement, the pump laser energy was fixed at 8.5 mJ. The seed pulse energy was less than 1 nJ and we estimated the absolute value with a calibrated photodiode. Due to the large bandwidth of the seeding pulse, only a small portion of the seeding pulse spectrum is amplified (Fig. 3 (a)). We therefore calculated the effective seeding pulse energy by considering the spectrum portion contained in the 1.06 nm bandwidth of the amplified 337 nm radiation. The maximum output amplified radiation at 337 nm was measured to be 1.2 nJ. This output pulse energy corresponds to an energy conversion efficiency of 1.4×10^{-7} from 8.5 mJ pump pulses. Therefore, the pulse energy of the ASE was deduced to be ~ 0.03 nJ based on the enhancement factor of 40, which gives a conversion efficiency of 3.5×10^{-9}. In the next section, we will estimate the corresponding laser intensity and show that it is less than the saturation laser intensity of the amplifier.
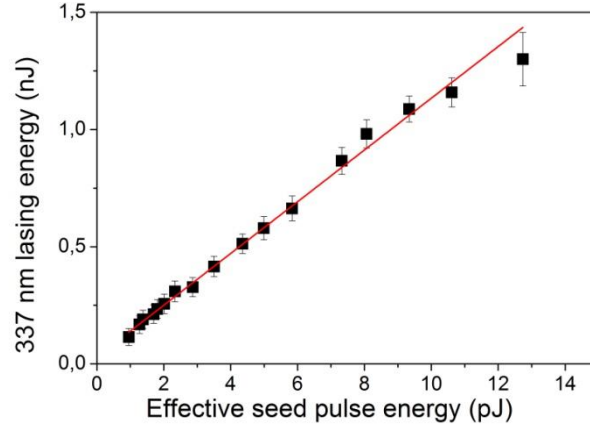
Fig. 6. Energy of the amplified 337 nm emission in the backward direction as a function of the seed pulse energy.

3.5 Pump laser polarization dependence of the amplified 337 nm laser

All the above experimental observations highlight the crucial role of pump laser polarization. To evaluate that, we measured systematically the 337 nm laser emission intensity by rotating the $\lambda/4$ waveplate for the pump pulses. In Fig. 7 (a), the result for the backward ASE is first presented as a function of the rotation angle ϕ of the waveplate, which has been reported in our previous work [7]. Intense ASE was observed only with circularly polarized pump pulses and shows dramatic decrease when the ellipticity deviates from $\varepsilon = 1$. In the presence of a constant linearly polarized seeding pulse, a similar dependence on laser ellipticity was observed (Fig. 7 (b)). This confirms that population inversion between the $C^3\Pi_u$ and $B^3\Pi_g$ states can be only achieved with circularly polarized pump pulses. The slight asymmetry and the deviation of the peaks from $\phi = 135°$ and $\phi = 315°$ can be due to the fact that the circularly polarized pump pulses reflect on the dielectric dichromatic mirror in this experiment. This mirror has slightly different reflectivity for p- and s- polarized light and thus results in a non-perfect circularly polarized pump pulses after reflection.
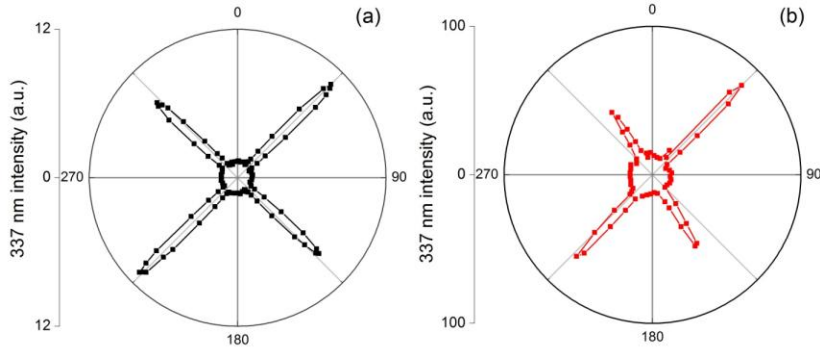

Fig. 7. Dependence of the backward ASE (a) and the seeded backward stimulated radiation (b) as a function of the rotation angle of the quarter-wave plate. The angles $\varphi = 90° \times m$ correspond to linearly polarized laser, with $m = 0, 1, 2, 3$. The angles $\varphi = 45° + 90° \times m$ correspond to circularly polarized laser.

3.6 Temporal characterization of the backward emission and the gain

In order to obtain temporal information such as pulse duration of the emission, we have tried to measure both the ASE and the amplified 337 nm emission with a fast photodiode (ALPHALAS, UPD-200-SP, rise time: 175 ps, bandwidth: 2GHz) connected to 13 GHz

oscilloscope (Agilent, model: Infiniium DSO91304A). We first tested the temporal response of this detection system with the femtosecond pulse, which serves as an impulse excitation. An oscilloscope trace with a width of ~ 500 ps is observed, reflecting the bandwidth limit of the photodiode. We then used this system to examine the duration of the ASE and the amplified 337 nm emission. In both cases, we observed no change of the signal width on the oscilloscope compared to the femtosecond pulse excitation. This suggests that the durations of the backward ASE and the amplified emission are less than 500 ps. To get precise knowledge of the pulse duration, optical methods such as cross-correlation are needed in the future study.

The temporal dynamic of the gain is very important aspect for an optical amplifier. With a seed pulse in the counter-propagation direction, displacement of the optical delay line changes the position of temporal overlapping between the pump and seed pulse. Therefore, we employed a co-propagation configuration to measure the gain dynamics, similar to that reported in ref. 8. We presented the results in Fig. 8 for three different nitrogen pressures. The zero temporal delay is defined as the position where noticeable amplification of the seeding pulse is observed. For 1 bar nitrogen gas, a gain built-up time of ~ 4 ps and a decay process of ~ 20 ps are observed. For decreased gas pressure of 600 and 400 mbar, the gain built-up time increases to 7 and 11 ps. This dependence of the gain built-up time on gas pressure supports our hypothesis of collisionally pumped population inversion, which will be further discussed later. We will also show in the discussion section that this relatively short gain lifetime has a fundamental influence on the amplification process and sets limit for the duration of the backward ASE. In the following analysis, we will take the effective lifetime (Full Width at Half Maximum, FWHM) of the gain τ_g to be ~ 15 ps.
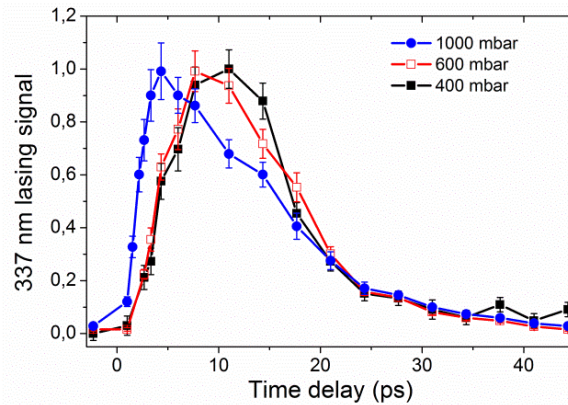

Fig. 8. Measured forward amplified 337 nm lasing signal as a function of the time delay between the pump and the seeding pulse. The pump pulse energy was 7.5 mJ.

3.7 Experiment in ambient air

The results presented above were obtained in pure nitrogen. We have previously found that the presence of oxygen molecules deteriorates the backward ASE [7]. In this seeded lasing scheme, we have tried to observe the amplification of the seed pulse propagating in both forward (co-propagation) and backward (counter-propagation) directions. For focal lens of $f = 1000$ mm, we observed almost no amplification of the seed pulse in ambient air in both co-propagation and counter-propagation configuration (Fig. 9 (a) and (b)).

In the work of Yao *et al*, the authors used an $f = 300$ mm lens and observed an amplification of ~ 2 times in atmospheric air [8]. We therefore tested a shorter focal lens of 500 mm in our experiments. In the co-propagation scheme, we observed an amplification of ~ 90 of the seeding pulse in ambient air (Fig. 9 (c)). This observation confirms that optical gain can be achieved in atmosphere with optimized pump conditions, which is very important for the future application of BLACK in atmospheric environment. However, in the counter-propagation configuration, we have observed no amplification. The optical gain of air plasma

amplifier is estimated to be $g = \ln(I_f / I_0)/l = 1.2$ cm^{-1}, with $l = 3$ cm the length of the plasma amplifier. With such a relatively weak gain of ~ 1.2 cm^{-1}, the amplification factor for the backward ASE can be approximated as $\exp(g l_{eff}) \sim 1.7$, with $l_{eff} = c\tau_g \sim 0.45$ cm the effective length of the amplifier for a backward propagating photon. Therefore, no significant amplification of the spontaneous emission photon should be expected in the backward direction with such un-sufficient gain, which agrees with our above observation.
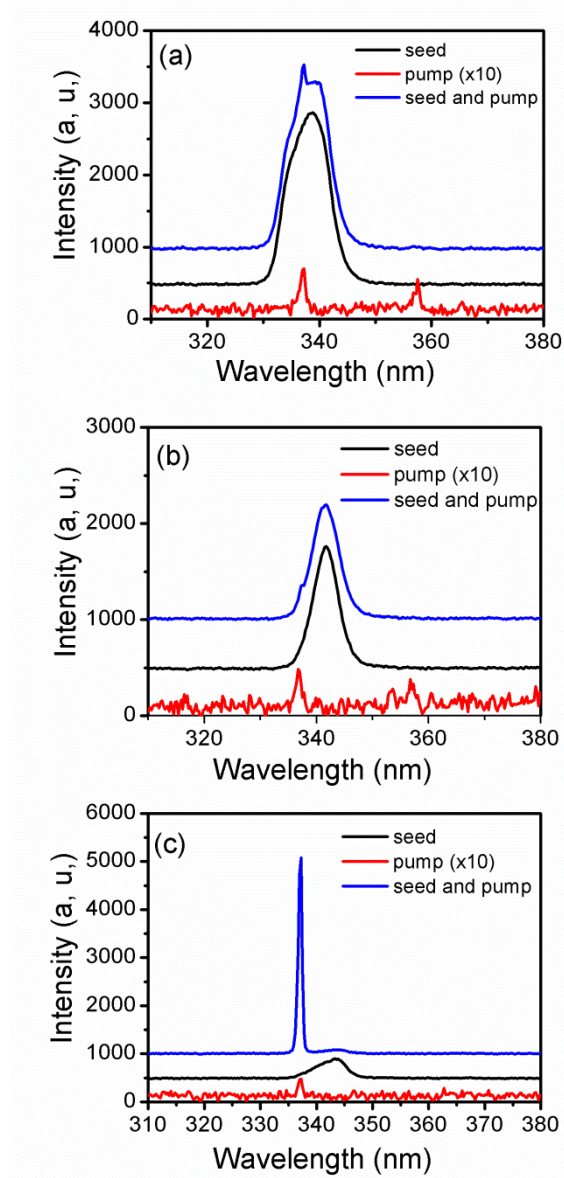

Fig. 9. Amplification of the seed pulse in atmospheric air. In (a) and (b), the seed pulse co-propagates and counter-propagates with respect to the pump pulses respectively. The focal lens was 1000 mm. In (c), the seed and the pump pulses were in the same direction and the focal lens was of $f = 500$ mm.

In our current study, the optical gain achieved in air is much less than that in pure nitrogen. The detrimental role of oxygen molecules has been attributed to the collision quenching

process and the decreased laser intensity inside the filaments due to the lower ionization potential of the oxygen molecules [7, 8]. Another possible process is the attachment of electrons to the neutral oxygen molecules [20], which can decrease the electron density.

We noticed that in the work of D. Kartashov and coworkers, the authors reported that the forward 337 nm lasing emission obtained in pure nitrogen were essentially identical to those in ambient air [13]. In this study, they employed linearly polarized picoseconds (2-10ps), 10 J pulses at 1.053 μm as pump pulse. The authors pointed out that no forward lasing action at 337 nm can be observed when the pulse duration becomes less than a threshold value of 2 ps. In our current study and that of Yao *et al*, femtosecond pulses with duration of ~ 40 fs were used. The different roles of oxygen molecules may be related to these distinct experimental parameters. A further study on this point is highly necessary, especially for the sake of future application of this backward 337 nm laser pumped by circularly polarized femtosecond pulses.

4. Further discussion

4.1 Mechanism for population inversion

In our previous work, we have attributed the population inversion to the following inelastic collision process:

$$N_2(X^1\Sigma_g^+) + e = N_2(C^3\Pi_u^+) + e.$$
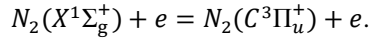
The effectiveness of circular laser polarization for population inversion lies in the fact that photoelectrons generated in a circularly polarized laser field are left with a substantial kinetic energy after the passage of the pump laser pulse. In our case of laser intensity around $1.4 \times 10^{14}\,\text{W/cm}^2$ [7], most of the electrons obtain kinetic energy around 16 eV, which is sufficiently high to excite the ground state nitrogen molecules to the third triplet state through inelastic collisions [21].

The measurement of the gain dynamics supports this hypothesis of population inversion. A gain built-up time of ~ 4-11 ps is clear in Fig. 8, which agrees well with the fact that the electron-molecules mean collision time is around 0.3 ps at atmospheric pressure. With decreased nitrogen pressures, the gain built-up time increases gradually due to the reduced collision frequency.

We would like to point out that population inversion by energetic electron collisions achieved with circularly polarized femtosecond pulses has been well developed in the domain of X-ray laser [22-26]. As first proposed by Corkum and Burnett in 1988, the hot electron distribution released by a circularly polarized laser field can be suitable to pump the upper level of laser transition by collision excitation [22]. Since then, numerous experimental demonstrations of X-ray laser in the ASE regime or seed-amplification regime have been reported, with a circularly polarized pump pulse [23-26]. For example, with a circularly polarized 30 fs, 1 J pump pulse, Ph. Zeitoun *et al* have demonstrated a small-signal gain coefficient of 80 cm^{-1} at 32.8 nm based on the optical transition of Kr^{8+} [23].

4.2 Pulse duration, laser intensity of the backward ASE

In a swept-gain amplifier such the filamentary plasma here, the pump pulse travels from one end of the amplifier to the other and the population inversion is built up sequentially inside the medium. The pulse duration of the backward ASE is related to three basic factors. The first factor concerns the spectrum bandwidth of the laser emission, which limits the pulse duration by Fourier transformation. The bandwidth of the 337 nm lasing was well known to be of ~ 0.1 nm, which corresponds to a Fourier transform limited pulse duration of ~ 2 ps. The second factor is the gain lifetime. The duration of the radiation emitted from a small segment ($\Delta z << c\tau_g$) of the amplifier should be less than the gain lifetime, beyond which no amplification is present. In our experiments, the gain lifetime has been measured to be around ~ 15 ps. The third factor is the traveling time of the pump pulse through the amplifier, which

is given by $\tau_t = l/c$. This corresponds to 100 ps for a 3 cm long plasma filament, which is much longer than the gain lifetime and the Fourier transform limited duration. The real pulse duration of the backward ASE can be estimated as the convolution of the above three characteristic times. Since the traveling time is much larger than the other two, the pulse duration of the backward ASE should be close to the pump traveling time $\tau_t \sim 100$ ps.

With a calibrated maximum pulse energy of 0.03 nJ, the power of the ASE emission can be estimated as $P = E_{ASE}/\tau_p \sim 0.3$ W. We have previously measured that the transverse diameter of the plasma amplifier is around 300 μm with similar experimental parameters [7]. Therefore, the laser intensity of the 337 nm ASE is $I_{ASE} = E_{ASE}/\pi\tau_p (d/2)^2 \sim 3.5 \times 10^2$ W/cm^2. The saturation intensity of the $C^3\Pi_u \rightarrow B^3\Pi_g$ transition is given by $I_{sat} = h\omega/2\pi\sigma_s T_C (1-v_{e,N_2}^B/v_{e,N_2}^B)$, where ω, σ_s, T_C, v_{e,N_2}^B, v_{e,N_2}^C are the frequency of the 337 nm emission, the cross-section of stimulated emission, the lifetime of the upper level $C^3\Pi_u$ state, the temperature-dependent excitation rates to the $C^3\Pi_u$ and $B^3\Pi_g$ states by electron collisions, respectively [5 , 6]. For $T_e \sim 16$ eV, we found $v_{e,N_2}^B \sim 0.7\times10^{-17}$ cm^{-2} and $v_{e,N_2}^B \sim 2\times10^{-17}$ cm^{-2} [27]. With $\sigma_s \sim 10^{-14}$ cm^2 and $T_C \sim 0.6$ ns [5, 6], we obtain $I_{sat} \sim 1.5\times10^7$ W/cm^2. The above estimated laser intensity I_{ASE} is 5 orders of magnitude less than the saturation intensity.

4.3 Pulse duration, laser intensity of the backward amplified 337 nm laser
In the presence of a backward seed pulse, we have observed a strong energy amplification of the seed pulse inside the plasma medium (Fig. 3 and Fig. 6). The pulse duration of our seed pulse is estimated to be around ~ 100 fs, taking into consideration of the dispersion of the 20 mm fused silica sample and other transmission optical elements such as the two lenses (L$_2$ and L$_3$) and the incident window. Due to the narrow bandwidth (~ 0.1 nm) of the optical gain, such a relatively broadband (~ 10 nm) seed pulse cannot be amplified uniformly in the spectrum domain. The bandwidth of the final output pulse is expected to be close to the bandwidth of the optical gain, $i.$ $e.$ ~ 0.1 nm. In analogy to the plasma amplifier seeded by large bandwidth high order harmonics for intense X-ray laser, we expect the output pulse in our case consists of the amplified seed pulse, a wake field with a complex structure related to Rabi oscillations and coherent decay, and the residual ASE [25, 26]. The temporal scale of the entire output pulse is found to be on the order of the gain lifetime [25, 26]. Therefore, a pulse duration of ~10 ps should be a good approximation for the amplified 337 nm radiation in our experiments. Considering the maximum pulse energy of 1.2 nJ, the peak power is found to be 1.2×10^2 W. The corresponding laser intensity inside the amplifier is then estimated to be 1.7 $\times 10^5$ W/cm^2, which is ~ 1 % of the saturation intensity. A better understanding of this amplification process can be achieved with numerical simulation of this collisionally pumped plasma amplifier, which is under progress at this moment.

5. Conclusion

In conclusion, we demonstrated that a seed pulse at 337 nm injected into the backward direction of the plasma filaments, which is generated in nitrogen gas pumped by circularly polarized 800 nm femtosecond laser pulses, can be amplified by a factor of ~ 200. The amplified lasing radiation inherits the polarization property of the seed pulse and its divergence angle was found to be around 3.8 mrad, much less than that of the backward ASE. The critical role of pump laser polarization was also observed in the seeded lasing regime, where intense lasing effect was only possible for circularly polarized pump pulses. The amplification phenomenon, the reduced divergence of the seeded lasing radiation, and the critical role of pump laser polarization confirms unambiguously the presence of population inversion between the $C^3\Pi_u$ and $B^3\Pi_g$ states of neutral N$_2$ molecules in the filament plasma. We attributed the population inversion mechanism to the collisions between the ground state neutral nitrogen molecules with energetic electrons, which is produced by the circularly

polarized femtosecond laser pulses during ionization. We also point out that this collisionally pumped population inversion scheme has been well developed in the domain of X-ray laser since 1990s.

We measured the temporal dynamics of the optical gain and found a pressure-dependent gain built-up time of 4 ~11 ps, and a gain lifetime of ~ 15 ps. In a swept-gain plasma amplifier, this gain lifetime is one order of magnitude less than the pump traveling time through the ~ 30 mm long plasma column. As a result, the pulse duration of the backward ASE is largely determined by the pump traveling time. With the measured maximum pulse energy of 0.03 nJ, we estimated the 337 nm ASE laser intensity is about 3.5×10^2 W/cm^2, which is 5 orders of magnitude less than the saturation laser intensity.

In the presence of a backward injected seed pulse, the maximum 337 nm pulse energy reaches 1.2 nJ. The small-signal gain was estimated to be 11.8 cm^{-1}. With estimated pulse duration of ~ 10 ps, the laser intensity was found to be 1.7×10^5 W/cm^2, which is about 1 % of the saturation intensity.

Finally, we demonstrated that optical gain at 337 nm can be achieved in plasma created in ambient air, by properly optimizing the focusing geometry of the pump pulses. This observation suggests the feasibility of BLACK in atmospheric environment for future applications.

Acknowledgments